

1 **The pluripotent stem cell-specific transcript ESRG is dispensable for human pluripotency**

2

3 Kazutoshi Takahashi^{1, 2, *}, Michiko Nakamura¹, Megumi Narita¹, Akira Watanabe³, Mai Ueda¹, Yasuhiro
4 Takashima¹, Shinya Yamanaka^{1, 2, 4}

5

6 ¹Department of Life Science Frontiers, Center for iPS Cell Research and Application, Kyoto University,
7 Kyoto, Japan

8 ²Gladstone Institute of Cardiovascular Disease, San Francisco, California, United States of America

9 ³Graduate School of Medicine, Kyoto University, Kyoto, Japan

10 ⁴Department of Anatomy, University of California, San Francisco, San Francisco, California, United States
11 of America

12

13 *Corresponding Author

14 E-mail: kazu@cira.kyoto-u.ac.jp

15

16 **Abstract**

17 Human pluripotent stem cells (PSCs) express human endogenous retrovirus type-H (HERV-H), which
18 exists as more than a thousand copies on the human genome and frequently produces chimeric
19 transcripts as long-non-coding RNAs (lncRNAs) fused with downstream neighbor genes. Previous
20 studies showed that HERV-H expression is required for the maintenance of PSC identity, and aberrant
21 HERV-H expression attenuates neural differentiation potentials, however, little is known about the actual
22 of function of HERV-H. In this study, we focused on ESRG, which is known as a PSC-related HERV-H-
23 driven lncRNA. The global transcriptome data of various tissues and cell lines and quantitative expression
24 analysis of PSCs showed that ESRG expression is much higher than other HERV-Hs and tightly silenced
25 after differentiation. However, the loss of function by the complete excision of the entire ESRG gene body
26 using a CRISPR/Cas9 platform revealed that ESRG is dispensable for the maintenance of the primed
27 and naïve pluripotent states. The loss of ESRG hardly affected the global gene expression of PSCs or
28 the differentiation potential toward trilineage. Differentiated cells derived from ESRG-deficient PSCs
29 retained the potential to be reprogrammed into induced PSCs (iPSCs) by the forced expression of
30 OCT3/4, SOX2, and KLF4. In conclusion, ESRG is dispensable for the maintenance and recapturing of
31 human pluripotency.

32

33 **Introduction**

34 Human pluripotent stem cells (PSCs) express several types of human endogenous retroviruses (HERV)
35 [1-3]. The HERV type-H (HERV-H) family is a primate-specific ERV element that was first integrated into
36 new world monkeys. During further primate evolution, this family's major expansion occurred before the
37 branch of old world monkeys [4]. The typical structure of a HERV-H consists of an interior component,
38 HERVH-int, flanked by two long terminal repeat 7 (LTR7), which have promoter activity [5, 6]. Recent
39 studies have demonstrated that the activity of LTR7 is highly specific in established human PSCs and
40 relatively absent in early human embryos. In contrast, other LTR7 variants such as LTR7B, C, and Y are
41 activated in broad types of early human embryos from the 8-cell to epiblast stages [7].

42 The importance of HERV-Hs in human PSCs has been shown. The knockdown of pan HERV-Hs using
43 short hairpin RNAs (shRNAs) against conserved sequences in LTR7 regions revealed that HERV-H
44 expression is required for the self-renewal of human PSCs [8, 9] and somatic cell reprogramming toward
45 pluripotency [8-14]. In addition to the self-renewal, the precise expression of HERV-Hs is crucial for the
46 neural differentiation potential of human PSCs [10, 15]. In this way, HERV-H expression contributes to
47 PSC identity.

48 The transcription of HERV-H frequently produces a chimeric transcript fused with a downstream neighbor
49 gene, which diversifies HERV-H-driven transcripts. Therefore, many HERV-H-driven RNAs contain
50 unique sequences aside from HERV-H consensus sequences. Indeed, PSC-associated HERV-H-
51 containing long non-coding RNAs (lncRNAs) have been reported [15-17]. One of them, ESRG (embryonic
52 stem cell-related gene; also known as HESRG) was identified as a transcript that is predominantly
53 expressed in undifferentiated human embryonic stem cells (ESCs) [18, 19]. ESRG is transcribed from
54 HERV-H LTR7 promoter [8, 20] and is activated in an early stage of somatic cell reprogramming induced
55 by the forced expression of OCT3/4, SOX2, and KLF4 (OSK) [12, 13, 20]. One previous study showed
56 that the short hairpin RNA (shRNA)-mediated knockdown of ESRG induces the loss of PSC characters
57 such as colony morphology and PSC markers along with the activation of differentiation markers,
58 suggesting the indispensability of ESRG for human pluripotency [8]. However, despite these
59 characterizations, the function of ESRG is still unknown.

60 In this study, we completely deleted ESRG alleles to analyze ESRG function in human PSCs with no off-
61 target risk. Surprisingly, the loss of ESRG, which is thought to be an essential lncRNA for PSC identity,
62 exhibited no impact on the self-renewal or differentiation potentials of both primed and naïve human
63 PSCs. Neural progenitor cells (NPCs) derived from ESRG-deficient PSCs could be reprogrammed into
64 induced PSC (iPSC) by OSK expression. This study revealed that ESRG is dispensable for human
65 pluripotency.

66
67

68

Results

69

ESRG is robustly expressed in PSCs and tightly silenced after differentiation

70

The RNA sequencing (RNA-seq) and chromatin immunoprecipitation (ChIP-seq) of histone H3 modifications indicated that the ESRG locus is open and actively transcribed in human PSCs but not in differentiated cells such as human dermal fibroblasts (HDFs) (Fig. 1A). As well as other HERV-H-related genes, LTR7 elements in ESRG gene are occupied by pluripotency-associated transcription factors (TFs) such as OSK [9, 10] (Fig. 1A). Little or no ESRG expression was detected in 24 adult tissues and five fetal tissues (Fig. S1A). Compared to other PSC-associated HERV-H chimeric transcripts, ESRG expression exhibits a sharp contrast between PSCs and somatic tissues [8, 10, 15-17]. Furthermore, ESRG is expressed in PSCs, including embryonic carcinoma cell (ECC) lines, but is silenced in four cancer cell lines and ten cell lines derived from normal tissue (Fig. S1B). Quantitative reverse transcription-polymerase chain reaction (qRT-PCR) revealed that the ESRG expression is significantly higher than the expression of other HERV-H-related transcripts and is comparable to the expression of SOX2 and NANOG, which play essential roles in pluripotency (Fig. 1B). These data suggest that ESRG expression is abundant in PSCs and is tightly silenced in differentiated states.

83

84

ESRG is dispensable for human pluripotency

85

The above results led us to hypothesize the important role of ESRG in human PSCs. To make a complete loss of function of the lncRNA ESRG, we employed a CRISPR/Cas9 platform and two single guide RNAs (sgRNAs) that flanked ~8,400 bp of the genomic region including the entire ESRG gene based on the human genome database and RNA-seq data (Figs. 1A and S2A). As a result, we obtained multiple independent ESRG knockout (KO) PSC lines that exhibit complete deletion of the gene body with unique minor deletion patterns in both alleles under a primed PSC culture condition (Figs. S2B and S2C). In this study, we used three clones as wild-type (WT) controls carrying intact ESRG alleles with no or minor deletions at the sgRNA recognition sites (Fig. S2D). We performed all subsequent experiments in 3 WT versus 3 KO manner. The expression of ESRG was undetectable in the KO clones by qRT-PCR (Fig. 1C). Immunocytochemistry showed that ESRG KO PSCs express the PSC core transcription factors (Fig. 1D) and PSC-specific surface antigens (Fig. 1E). The loss of ESRG made no impact on the expression of neighbor genes located within 10 Mbp of ESRG (Fig. 1F). Global transcriptome analysis revealed that the loss of ESRG altered the expression of only a few genes (Fig. 1G). Moreover, ESRG KO PSCs normally survived while maintaining the undifferentiated state as judged by alkaline phosphatase (AP) activity and the absence of any apparent genomic abnormalities (Figs. 1H and S3). These data suggest that ESRG is dispensable for the self-renewing of primed PSCs.

101

102

We also tested if ESRG is required for another state of pluripotency, the so-called naïve state, which also expresses ESRG but at a significantly lower level than the primed state (Fig. 2A). Regardless of the

103 ESRG expression, naïve PSCs could be established by switching the media composition and could self-
104 renew while keeping a tightly packed colony formation (Fig. 2B) [21-23]. Furthermore, they exhibited a
105 significantly high expression of the naïve pluripotency markers KLF4 and KLF17 and attenuated the
106 expression of the primed PSC marker ZIC2 (Fig. 2C) [24, 25]. Microarray analysis revealed that ESRG
107 had no effect on the global gene expression of either primed or naïve PSCs (Fig. 2D). We also
108 differentiated ESRG WT and KO naïve PSCs to the primed pluripotent state. As a result, irrespective of
109 the ESRG genotype, we detected the hallmarks of primed pluripotency such as flatter colony formation,
110 the reactivation of ZIC2 and the suppression of KLF4 and KLF17, suggesting the bidirectional transition
111 between naïve and primed pluripotency does not require ESRG (Figs. 2E and 2F). Taken together, these
112 data demonstrate that ESRG is dispensable for the maintenance of human PSCs.

113

114 **ESRG is not involved in differentiation**

115 Next, we analyzed whether ESRG is required for the differentiation of PSCs by embryoid body (EB)
116 formation. The absence of ESRG had no effect on EB formation by floating culture or differentiation into
117 trilineage such as alpha-fetoprotein (AFP) positive (+) endoderm, smooth muscle actin (SMA) (+)
118 mesoderm and β III-TUBULIN (+) ectoderm (Figs. 3A and 3B). Other lineage markers such as DCN
119 (endoderm), MSX1 (mesoderm) and MAP2 (ectoderm) were also well induced in EBs derived from either
120 ESRG WT or KO PSCs (Fig. 3C). Global transcriptome analysis by microarray indicated the loss of ESRG
121 caused no significant gene expression changes during EB differentiation (Fig. 3D). These data suggest
122 that ESRG KO PSCs retained the potential to differentiate into all three germ layers.

123 Previous studies showed that HERV-H expression regulates the neural differentiation potential of human
124 PSCs [10, 15, 26]. Thus, in addition to the random differentiation by EB formation, we tested whether
125 ESRG contributes to the directed differentiation of PSCs into NPCs by the dual SMAD inhibition method
126 [27, 28]. Both ESRG WT and KO PSCs were able to differentiate into expandable NPCs, which expressed
127 the early neural lineage marker PAX6 but not OCT3/4 (Fig. 3E). Other NPC markers such as SOX1 and
128 NES were well induced, whereas the PSC marker NANOG was silenced (Fig. 3F). These data suggest
129 that ESRG is not responsible for HERV-H-regulated neural differentiation. Taken together, we concluded
130 that ESRG is not required for the differentiation of human PSCs.

131

132 **ESRG is not required for somatic cell reprogramming toward pluripotency**

133 A previous study showed that the overexpression of ESRG improves iPSC generation [8], suggesting a
134 positive effect on somatic cell reprogramming toward pluripotency. The activation of ESRG in the early
135 stage of reprogramming and the high expression of ESRG during reprogramming support this hypothesis
136 (Fig. 4A) [20]. Therefore, we reprogrammed ESRG WT and KO NPCs to iPSCs by introducing OSK.
137 iPSCs emerged from ESRG WT and KO NPCs with comparable efficiency (Fig. 4B). This observation

138 suggests that ESRG is dispensable for iPSC generation. In addition, along with OSK, we transduced c-
139 MYC, a potent enhancer of iPSC generation [29, 30], or exogenous ESRG. c-MYC but not exogenous
140 ESRG increased the efficiency of the iPSC generation from ESRG WT and KO NPCs equally (Fig. 4B).
141 Taken together, these data suggest that ESRG has no impact on somatic cell reprogramming toward
142 iPSCs.

143

144

145 **Discussion**

146 In this study, we completely excised the entire ESRG gene to understand its role in human PSCs while
147 avoiding residual expression and off-target effects. Unexpectedly, ESRG KO PSCs showed no apparent
148 phenotypes in self-renewal or differentiation potential. A previous study showed the importance of ESRG
149 in human PSC identity by using an shRNA-mediated knockdown approach [8]. Although we used the
150 same H9 ESC line as that study, the different strategies for the loss of function and subsequent
151 experiments, such as knockdown and knockout, may explain the different results. For example, the speed
152 of the loss of function may differ. Generally, RNA interference (RNAi) induces acute silencing of the target
153 gene expression, whereas the knockout process is relatively slow and has multiple stages, including
154 CRISPR/Cas9-mediated deletion, clonal expansion, subcloning and others. Another possibility is the off-
155 target effect of RNAi. Similar observations have been found for the role of lncRNA Cyrano that is highly
156 conserved in mouse and human. Knockdown by using shRNA suggested Cyrano lncRNA maintains
157 mouse PSC identity [31], but targeted deletion of the Cyrano gene and gene silencing by CRISPR
158 interference demonstrated no impact on mouse or human PSC identity [32-34]. Further, it has been
159 argued that the shRNA-mediated knockdown of nuclear lncRNAs might be difficult or inefficient compared
160 to cytoplasmic RNAs such as mRNAs [35, 36]. In addition, while small nucleotide insertions or deletions
161 causing frameshift of the reading frames work well for the loss of function of protein-coding genes, the
162 same is not true for non-coding RNAs. In this context, our study succeeded to generate the complete
163 deletion of ESRG gene alleles, providing highly reliable results.

164 This study clearly demonstrated that ESRG is dispensable for human PSC identity. Neither primed nor
165 naïve PSCs require ESRG for their identities, such as colony morphology or gene expression signatures,
166 meaning ESRG is dispensable for human pluripotency, at least in an in vitro culture environment.
167 However, since ESRG is expressed in epiblast-stage human embryos [8, 37], it might be involved in early
168 human embryogenesis.

169 ESRG is stochastically activated by OSK in rare reprogrammed intermediates that have the potential to
170 become bona fide iPSCs and is highly expressed throughout the process of reprogramming toward iPSCs
171 [20]. In the present study, we showed that ESRG KO NPCs can be reprogrammed with the same
172 efficiency as ESRG WT NPCs. These data suggest that ESRG is a good marker of the intermediate cells

173 in early stage of reprogramming rather than a functional molecule that is need for iPSC generation.
174 In summary, this study provides clear evidence of the dispensability of ESRG for PSC identities, such as
175 global gene expressions and differentiation potentials, in two distinct types of pluripotent states. We also
176 demonstrated that the function of ESRG is not required for recapturing pluripotency via somatic cell
177 reprogramming. Finally, the tightly regulated and high expression of ESRG promises to make an excellent
178 marker of undifferentiated PSCs both in basic research and clinical application [20, 38].
179
180

181 **Methods**

182 **The culture of primed PSCs** | H9 ESC (RID:CVCL_9773) and 585A1 iPSC (RRID:CVCL_DQ06) lines
183 were maintained in StemFiT AK02 media (Ajinomoto) supplemented with 100 ng/ml recombinant human
184 basic fibroblast growth factor (bFGF, Peprotech) (hereafter F/A media) on a tissue culture plate coated
185 with Laminin 511 E8 fragment (LN511E8, NIPPI). A 201B7 iPSC (RRID:CVCL_A324) line was cultured
186 on mitomycin C (MMC)-inactivated SNL mouse feeder cells (RRID:CVCL_K227) in Primate ESC Culture
187 medium (ReproCELL) supplemented with 4 ng/ml bFGF.

188

189 **Induction and maintenance of naïve PSCs** | The conversion of primed PSCs to the naïve state was
190 performed as described previously [23]. Prior to naïve conversion, primed PSCs were maintained on
191 MMC-treated primary mouse embryonic fibroblasts (PMEFs) in DFK20 media consisting of DMEM/F12
192 (Thermo Fisher Scientific), 20% Knockout Serum Replacement (KSR, Thermo Fisher Scientific), 1%
193 MEM non-essential amino acids (NEAA, Thermo Fisher Scientific), 1% GlutaMax (Thermo Fisher
194 Scientific) and 0.1 mM 2-mercaptoethanol (2-ME, Thermo Fisher Scientific) supplemented with 4 ng/ml
195 bFGF. The cells were harvested using CTK solution (ReproCELL) and dissociated to single cells. One
196 hundred thousand cells were plated onto MMC-treated PMEFs in a well of a 6-well plate in DFK20 media
197 plus bFGF and 10 μ M Y-27632. Thereafter, the cells were incubated in hypoxic condition (5% O₂). On the
198 next day, the media was replaced with NDiff227 (Takara) supplemented with 1 μ M PD325901 (Stemgent),
199 10 ng/ml of recombinant human leukemia inhibitory factor (LIF, EMD Millipore) and 1 mM Valproic acid
200 (Wako). Three days later, the media was switched to PXGL media (NDiff227 supplemented with 1 μ M
201 PD325901, 2 μ M XAV939 (Wako), 2 μ M Gö6983 (Sigma Aldrich) and 10 ng/ml of LIF). When round shape
202 colonies were visible (around day 9 of the conversion), the cells were dissociated using TrypLE Express
203 (Thermo Fisher Scientific) and plated onto a new PMEF feeder plate in PXGL media plus 10 μ M Y-27632.
204 The media was changed daily, and the cells were passaged every 4-5 days. Cells after at least 30 days
205 of the conversion were used for the assays.

206

207 **Differentiation of naïve PSCs to the primed state** | Naïve PSCs were harvested using TrypLE Express
208 and plated at 5×10^5 cells onto a well of a LN511E8-coated 6-well plate in PXGL media supplemented
209 with 10 μ M Y-27632. On the next day, the media was replaced with F/A media. After 2 and 8 days, the
210 cells were harvested and split to a new LN511E8-coated plate in F/A media plus 10 μ M Y-27632. On day
211 16 of the differentiation, the cells were fixed for immunocytochemistry, and RNA samples were collected
212 to analyze the marker gene expression.

213

214 **Induction and maintenance of NPCs** | Primed PSCs were differentiated into expandable NPCs by using
215 the STEMdiff SMADi Neural Induction Kit (Stem Cell Technologies) as previously described [26-28]. In

216 brief, primed PSCs were maintained on a Matrigel (Corning)-coated plate in mTeSR1 media (Stem Cell
217 Technologies) prior to the NPC induction. The cells were harvested using Accutase (EMD Millipore) and
218 transferred at 3×10^6 cells to a well of an AggreWell800 plate (Stem Cell Technologies) in STEMdiff Neural
219 Induction Medium + SMADi (Stem Cell Technologies) supplemented with 10 μ M Y-27632. Five days later,
220 uniformly sized aggregates were collected using a 37 μ m Reversible Strainer (Stem Cell Technologies)
221 and plated onto a Matrigel-coated 6-well plate in STEMdiff Neural Induction Medium + SMADi. Seven
222 days later, neural rosette structures were selectively removed by using STEMdiff Neural Rosette
223 Selection Reagent (Stem Cell Technologies) and plated onto a new Matrigel-coated 6-well plate in
224 STEMdiff Neural Induction Medium + SMADi. After that, the cells were passaged every 2-3 days until day
225 30 post-differentiation. The established NPCs were maintained on a Matrigel-coated plate in STEMdiff
226 Neural Progenitor Medium (Stem Cell Technologies) and passaged every 3-4 days.
227

228 **The culture of other cells** | HDFs and PLAT-GP packaging cells (RRID:CVCL_B490) were cultured in
229 DMEM (Thermo Fisher Scientific) containing 10% fetal bovine serum (FBS, Thermo Fisher Scientific).
230

231 **Embryoid body (EB) differentiation** | PSCs were cultured on a Matrigel-coated plate in mTeSR1 media
232 until reaching confluence prior to EB formation. The cells were harvested using CTK solution
233 (ReproCELL), and cell clumps were transferred onto an ultra-low binding plate (Corning) in DFK20
234 media. For the first 2 days, 10 μ M Y-27362 was added to the media to improve cell survival. The media
235 was changed every other day. After 8 days of floating culture, the EBs were transferred onto a tissue
236 culture plate coated with 0.1% gelatin (EMD Millipore) and maintained in DFK20 media for another 8
237 days.
238

239 **Plasmid** | Full-length ESRG complementary DNA (cDNA) was amplified using ESRG-S and ESRG-AS
240 primers and inserted into the BamHI/NotI site of a pMXs retroviral vector [39] using In-Fusion technology
241 (Clontech). The primer sequences for the cloning are available in S1 Table.
242

243 **Reprogramming** | Retroviral transduction of the reprogramming factors was performed as described
244 previously [12, 20]. A pMXs retroviral vector encoding human OCT3/4 (RRID:Addgene_17217), human
245 SOX2 (RRID:Addgene_17218), human KLF4 (RRID:Addgene_17219), human c-MYC
246 (RRID:Addgene_17220) and ESRG (6 μ g each) along with 3 μ g of pMD2.G (gift from Dr. D. Trono;
247 RRID:Addgene_12259) was transfected into PLAT-GP packaging cells, which were plated at 3.6×10^6
248 cells per 100 mm dish the day before transfection, using FuGENE6 transfection reagent (Promega). Two
249 days after the transfection, virus-containing supernatant was collected and filtered through a 0.45 μ m-
250 pore size cellulose acetate filter to remove the cell debris. Viral particles were precipitated using Retro-X

251 Concentrator (Clontech) and resuspended in STEMdiff Neural Progenitor Medium containing 8 µg/ml
252 Polybrene (EMD Millipore). Then, appropriate combinations of viruses were mixed and used for the
253 transduction to NPCs. This point was designated day 0. The cells were harvested on day 3 post-
254 transduction and replated at 5 x 10⁴ cells per well of a LN511E8-coated 6-well plate in STEMdiff Neural
255 Progenitor Medium. The following day (day 4), the medium was replaced with F/A media, and the medium
256 was changed every other day. The iPSC colonies were counted on day 24 post-transduction. Bona fide
257 iPSC colonies were distinguished from non-iPSC colonies by their morphological differences and/or
258 alkaline phosphatase activity.

259

260 **Deletion of ESRG gene** | A ribonucleoprotein complex consisting of 40 pmol of Alt-R S.p. HiFi Cas9
261 Nuclease V3 (Integrated DNA Technologies) and two single guide RNAs (sgRNAs): sgESRG-U (5'-
262 AGAGAAUACGAAGCUAAGUG-3') and sgESRG-L (5'-AUUGCAGUUGUCACAUGACA-3'), 150 pmol
263 each; SYNTHEGO was introduced into 5 x 10⁵ H9 ESCs (passage number 49) from a subconfluent
264 culture using a 4D-Nucleofector System with X Unit (Lonza) and P3 Primary Cell 4D-Nucleofector Kit S
265 (Lonza) with the CA173 program. Three days after the nucleofection, the cells were harvested and
266 replated at 500 cells onto a LN511E8-coated 100 mm dish in F/A media supplemented with 10 µM Y-
267 27632. The cells were maintained until the colonies grew big enough for subcloning. The colonies were
268 mechanically picked up, dissociated using TrypLE select and plated onto a LN511E8-coated 12-well plate
269 in F/A media supplemented with 10 µM Y-27632.

270 The genomic DNA of the expanded clones was purified using the DNeasy Blood & Tissue Kit (QIAGEN).
271 Fifty nanograms of purified DNA was used for quantitative polymerase chain reaction (PCR) using
272 TaqMan Genotyping Master Mix (Thermo Fisher Scientific) on an ABI7900HT Real Time PCR System
273 (Applied Biosystems). TaqMan Assays (Thermo Fisher Scientific) such as ESRG_cn1 (Hs05898393_cn)
274 and ESRG_cn2 (Hs06675423_cn) detected the ESRG locus and TaqMan Copy Number Reference
275 Assay human RNase P (4403326, Thermo Fisher Scientific) was used as an endogenous control. To
276 verify the indel patterns in wild-type clones, fragment around the sgESRG-U and sgESRG-L recognition
277 sites were amplified with ESRG-U-S/ESRG-U-AS and ESRG-L-S/ESRG-L-AS primer sets, respectively.
278 The amplicons were purified using the QIAquick PCR Purification Kit (QIAGEN) and subjected to
279 sequencing. To check the deleted sequences in the knockout clones, a fragment with ESRG-U-S/ESRG-
280 L-AS primers was amplified. Conventional PCR was performed using KOD Xtreme Hot Start DNA
281 Polymerase (EMD Millipore). The fragments were cloned into pCR-Blunt II TOPO using the Zero Blunt
282 TOPO PCR Cloning Kit (Thermo Fisher Scientific), and the sequencing was verified using M13 forward
283 and M13 reverse universal primers. The sequence data was analyzed using SnapGene software (GSL
284 Biotech LLC). The primer sequences are provided in S1 Table.

285

286 **RNA isolation and reverse-transcription polymerase chain reaction** | The cells were lysed with
287 QIAzol reagent (QIAGEN), and the total RNA was purified using a miReasy Mini Kit (QIAGEN) according
288 to the manufacturer's protocol. The reverse transcription (RT) of 1 μ g of purified RNA was done by using
289 SuperScript III First-Strand Synthesis SuperMix (Thermo Fisher Scientific). Quantitative RT-PCR was
290 performed using TaqMan Assays with TaqMan Universal Master Mix II, no UNG (Applied Biosystems) on
291 an ABI7900HT or a QuantoStudio 5 Real Time PCR System (Applied Biosystems). The C_t values of the
292 undetermined signals caused by too low expression was set at 40. The levels of mRNA were normalized
293 to the GAPDH expression, and the relative expression was calculated as the fold-change from the control.
294 Information about the TaqMan Assays is shown in S2 Table.

295

296 **Gene expression analysis by microarray** | The total RNA samples were purified using the miReasy
297 Mini Kit, and the quality was evaluated using a 2100 Bioanalyzer (Agilent Technologies). Two hundred
298 nanograms of total RNA was labeled with Cyanine 3-CTP and used for hybridization with SurePrint G3
299 Human GE 8x60K (version 1 (G4851A) and version 3 (G4851C), Agilent Technologies) and the one-color
300 protocol. The hybridized arrays were scanned with a Microarray Scanner System (G2565BA, Agilent
301 Technologies), and the extracted signals were analyzed using the GeneSpring version 14.6 software
302 program (Agilent Technologies). Gene expression values were normalized by 75th percentile shifts.
303 Differentially expressed genes between ESRG WT and KO ESCs were extracted by t-tests with Benjamini
304 and Hochberg corrections [fold change (FC) > 2.0, false-discovery rate (FDR) < 0.05].

305

306 **Immunocytochemistry** | The cells were washed once with PBS, fixed with fixation buffer (BioLegend)
307 for 15 min at room temperature and blocked in PBS containing 1% bovine serum albumin (BSA, Thermo
308 Fisher Scientific), 2% normal donkey serum (Sigma-Aldrich) for 45 min at room temperature. For the
309 staining of intracellular proteins, the fixed cells were permeabilized by adding 0.2% TritonX-100 (Teknova)
310 during the blocking process. Then the cells were incubated with primary antibodies diluted in PBS
311 containing 1% BSA at 4°C overnight. After washing with PBS, the cells were incubated with secondary
312 antibodies diluted in PBS containing 1% BSA and 1 μ g/ml Hoechst 33342 (Thermo Fisher Scientific) for
313 45 min at room temperature in the dark. The fluorescent signals were detected using a BZ-X710 imaging
314 system (KEYENCE). The antibodies and dilution rate were as follows: anti-OCT3/4 (1:250, 611203, BD
315 Biosciences), anti-SOX2 (1:100, ab97959, Abcam), anti-NANOG (1:100, ab21624, Abcam), anti-KLF17
316 (1:100, HPA024629, Atlas Antibodies), anti-PAX6 (1:1,000, 901301, BioLegend), SSEA3 (1:100, 09-0044,
317 Stemgent), SSEA4 (1:100, 09-0006, Stemgent), SSEA5 (1:100, 355201, BioLegend), TRA-1-60 (1:100,
318 MAB4360, EMD Millipore), TRA-2-49/6E (1:100, 358702, BioLegend), anti-AFP (1:200, GTX15650,
319 GeneTex), anti-SMA (1:200, CBL171-I, EMD Millipore), anti- β III-TUBULIN (1:1,000, XMAB1637, EMD

320 Millipore), Alexa 488 Plus anti-mouse IgG (1:500, A32766, Thermo Fisher Scientific), Alexa 647 Plus anti-
321 rabbit IgG (1:500, A32795, Thermo Fisher Scientific), Alexa 594 anti-rat IgM (1:500, A21213, Thermo
322 Fisher Scientific) and Alexa 555 anti-mouse IgM (1:500, A21426, Thermo Fisher Scientific).

323

324 **Quantification and statistical analysis** | Data are presented as the mean \pm standard deviation unless
325 otherwise noted. Sample number (n) indicates the number of replicates in each experiment. The number
326 of experimental repeats is indicated in the figure legends. To determine statistical significance, we used
327 the unpaired t-test for comparisons between two groups using Excel Microsoft 365 (Microsoft). Statistical
328 significance was set at $p < 0.05$. All graphs and heatmaps were generated using GraphPad Prism 8
329 software (GraphPad).

330

331 **Data availability** | RNA-seq and ChIP-seq (GSE56569 and GSE89976) and Gene expression microarray
332 (GSE54848, GSE156834 and GSE159101) results are accessible in the Gene Expression Omnibus
333 database of the National Center for Biotechnology Information website.

334

335

336 **Acknowledgements**

337 We would like to thank M. Iwasaki, M. Koyanagi-Aoi, A. Kunitomi, K. Okita, M. Ohnuki and D. Trono for
338 sharing materials and data, MA. Khurram, SD. Perli, S. Wang and K. Tomoda for discussions, and Y.
339 Kawahara, M. Lancero and R. Hirohata for technical assistance. We are also grateful to K. Essex, K.
340 Higashi, K. Kamegawa, M. Otsuki, M. Saito and S. Takeshima for administrative support, and P.
341 Karagiannis for crucial reading of the manuscript.

342

343

344 **Funding**

345 This work was supported by Grants-in-Aid for Scientific Research (20K20585) from the Japanese Society
346 for the Promotion of Science (JSPS); a grant from the Core Center for iPS Cell Research
347 (19bm0104001h0007), Research Center Network for Realization of Regenerative Medicine from Japan
348 Agency for Medical Research and Development (AMED); a grant from the Japan Foundation for Applied
349 Enzymology; a grant from the Fujiwara Memorial Foundation; a grant from the Takeda Science
350 Foundation; and the iPS Cell Research Fund from Center for iPS Cell Research and Application, Kyoto
351 University. The study was also supported by funding from Mr. H. Mikitani, Mr. M. Benioff, and the L.K.
352 Whittier Foundation.

353

354

355 **Author contributions**

356 Conceptualization, K.T. and S.Y.; Methodology, K.T., M.U., and Y.T.; Investigation, K.T., M.Nakamura,
357 M.Narita, and A.W.; Formal Analysis, K.T and A.W.; Writing – Original Draft, K.T.; Funding Acquisition,
358 K.T. and S.Y.; Resources, K.T., M.U., and Y.T.; Supervision, K.T. and S.Y.

359

360

361 **Competing interests**

362 K.T. is on the scientific advisory board of I Peace, Inc. without salary. S.Y. is a scientific advisor (without
363 salary) of iPS Academia Japan. All other authors have no conflict of interest.

364

365

366 **Figure legends**

367 **Figure 1 | ESRG is dispensable for primed pluripotency**

368 (A) Epigenetic status of the ESRG locus. Shown are RNA-seq and ChIP-seq data for histone
369 modifications and PSC core transcription factor (TF) binding on the ESRG locus in HDFs and iPSCs on
370 human genome assembly hg19. The green arrowheads at the bottom indicate the location of the LTR7
371 elements. (B) Expression of PSC-associated mRNAs and HERV-H chimeric RNAs. Shown are the
372 averaged expressions of the indicated transcripts in H9 ESCs, 585A1 iPSCs and 201B7 iPSCs. Error
373 bars and white lines indicate min. to max. and the mean of each gene expression, respectively. Values
374 are compared to GAPDH. n=3. (C) Expression of ESRG in ESRG WT and KO PSC clones. Values are
375 normalized by GAPDH and compared with primed H9 ESCs. n=3. (D) Expression of PSC core
376 transcription factors. Bars, 100 μ m. (E) Expression of PSC-specific surface antigens. Bars, 100 μ m. (F)
377 Expression of neighbor genes <10 Mbp apart from ESRG gene. Values are normalized by GAPDH and
378 compared with parental primed H9 ESCs. n=3. (G) Global gene expression. Scatter plots compare the
379 microarray data of ESRG WT and KO primed PSCs. The colored plots indicate differentially expressed
380 genes (DEGs) with statistical significance (FC>2.0, FDR, 0.05). Number of DEGs are shown in the figure.
381 n=3. (H) Plating efficiency. Shown are the number of AP (+) colonies raised from 100 or 200 ESRG WT
382 and KO PSCs. n=3. Numerical values for B, C, F, and H are available in S1 Data.

383

384 **Figure 2 | No impact of ESRG on naïve pluripotency**

385 (A) The ESRG expression. Shown are relative expressions of ESRG in primed PSCs, naïve PSCs, NPCs
386 and HDFs. Values are normalized by GAPDH and compared with the primed 585A1 iPSC line. *P<0.05
387 vs. primed PSCs by unpaired t-test. n=3. (B) Conversion to naïve pluripotency. Shown are representative
388 images of ESRG WT and KO primed and naïve PSCs under phase contrast and of immunocytochemistry
389 for KLF17 (red) and OCT3/4 (green). Bars, 200 μ m. (C) The expression of primed and naïve PSC markers.
390 Shown are the relative expressions of common PSC markers (POU5F1 and NANOG), a primed PSC
391 marker (ZIC2) and naïve PSC markers (KLF4 and KLF17). Values are normalized by GAPDH and
392 compared with primed H9 ESCs. n=3. (D) Global transcriptome. Scatter plots comparing the microarray
393 data of ESRG WT and KO naïve PSCs. The colored plot indicates DEG with statistical significance
394 (FC>2.0, FDR,0.05). Number of DEGs are shown in the figure. n=3. (E) Differentiation to primed
395 pluripotency. Representative images of ESRG WT and KO naïve PSCs before and after conversion to
396 the primed pluripotent state are shown. Bars, 200 μ m. (F) The expression of primed and naïve PSC
397 markers. Shown are the relative expressions of the marker genes in (C) in ESRG WT and KO naïve
398 PSCs before and after the differentiation to the primed pluripotent state. Values are normalized by
399 GAPDH and compared with primed H9 ESCs. n=3. Numerical values for A, C, and F are available in S1
400 Data.

401

402 **Figure 3 | ESRG-deficient PSCs are capable of differentiating.**

403 (A) Differentiation by EB formation. Bars, 500 μ m. (B) Trilineage differentiation. Bars, 200 μ m. (C) The
404 expression of differentiation markers. Shown are the relative expressions of PSC markers (POU5F1 and
405 NANOG) and differentiation markers (DCN, MSX1 and MAP2) on days 8 and 16 of EB differentiation.
406 Values are normalized by GAPDH and compared with primed H9 ESCs. n=3. (D) Global gene expression
407 of differentiation derivatives. Scatter plots compare the microarray data of ESRG WT and KO PSC-
408 derived EBs on days 8 and 16. Number of DEGs (FC>2.0, FDR,0.05) are shown in the figure. n=3. (E)
409 NPC differentiation. Representative images of ESRG WT and KO PSCs and NPCs under phase contrast
410 and of immunocytochemistry for PAX6 (red) and OCT3/4 (green) are shown. Bars, 200 μ m. (F) The
411 expression of NSC markers. Shown are the relative expressions of PSC markers (POU5F1 and NANOG)
412 and NPC markers (PAX6, SOX1 and NES) in ESRG WT and KO PSCs and NPCs. Values are normalized
413 by GAPDH and compared with primed H9 ESCs. n=3. Numerical values for C and F are available in S1
414 Data.

415

416 **Figure 4 | ESRG is dispensable for iPSC reprogramming.**

417 (A) The expression of ESRG during reprogramming. The heatmap shows the normalized intensities of
418 ESRG, POU5F1 (endogenous), SOX2 (endogenous) and NANOG expression from microarray data in
419 the time course of iPSC reprogramming (days 0-49) and established iPSCs (far right). n=3. (B) The effect
420 of ESRG on iPSC generation. Shown are the numbers of AP (+) iPSC colonies 24 days after the
421 transduction of OSK along with Mock (n=4), ESRG (n=4) and c-MYC (n=5). Numerical values for A and
422 B are available in S1 Data.

423

424

425 **Supporting information**

426 **S1 Fig. ESRG expression profiles.** Expression of ESRG in human tissues. (A) Shown are the
427 normalized intensities of ESRG expression from the microarray data of PSCs (H9 ESC), 24 adult tissues
428 and five fetal tissues. (B) Expression of ESRG in human cell lines. The normalized intensities of ESRG
429 expression from the microarray data of several PSC lines including H9 ESC, 201B7 iPSC, 585A1 iPSC,
430 2102Ep embryonic carcinoma cells (ECC) and NTERA-2 ECC, cancer cell lines such as MCF7, HepG2,
431 HeLa and Jurkat, and normal tissue-derived cells such as adipose tissue-derived mesenchymal stem
432 cells (AdMSC), dental pulp-derived MSCs (DpMSC), human dermal fibroblasts (HDF), peripheral blood
433 mononuclear cells (PBMC), bronchial epithelial cells (BrEC), prostate epithelial cells (PrEC), hepatocytes
434 (Hep), epidermal keratinocytes (EKc), neural progenitor cells (NPC) and astrocytes (Astrocyte) are shown.
435 Numerical values for A and B are available in S1 Data.

436

437 **S2 Fig. Deletion of ESRG locus.** (A) The scheme of ESRG targeting. The locations of sgRNAs for
438 targeting (sgESRG-U and -L), primers for genotyping (U-S/AS and L-S/AS) and TaqMan Assays for copy
439 number analyses (cn1 and cn2) are shown. The sequences of sgRNAs and primers are provided in the
440 Methods section and S1Table. (B) The copy number of ESRG gene. The copy number of ESRG gene in
441 ESRG WT (clones 1, 21 and 28), a heterozygous clone (Het) that lacks one ESRG allele and KO (clones
442 10, 18 and 23) were quantified by qPCR using TaqMan Copy Number Assays (cn1 and 2). Values are
443 normalized by RNase P and compared with parental H9 ESCs. n=3. (C) The sequences around the
444 deletion sites in ESRG KO ESC clones verified by Sanger sequencing. (D) The sequences around the
445 sgRNA recognition sites upstream (sgESRG-U) and downstream (sgESRG-L) of the ESRG locus in
446 ESRG WT ESC clones verified by Sanger sequencing. Numerical values for B are available in S1 Data.
447

448 **S3 Fig. Karyotypes of PSC clones used in the study.** Representative images of G-band staining show
449 that all clones used in the study maintained normal female karyotypes (46XX).

450

451 **S1 Table. Primers used in this study.**

452

453 **S2 Table. TaqMan Assays used in this study.**

454

455 **S1 Data. In separate sheets, the excel spreadsheet contains the numerical values for Figs. 1B, 1C,
456 1F, 1H, 2A, 2C, 2F, 3C, 3F, 4A, and 4B; S1A, S1B and S2B Figs.**

457

458

459

460

References

1. Santoni FA, Guerra J, Luban J. HERV-H RNA is abundant in human embryonic stem cells and a precise marker for pluripotency. *Retrovirology*. 2012;9:111. Epub 2012/12/21. doi: 10.1186/1742-4690-9-111. PubMed PMID: 23253934; PubMed Central PMCID: PMC3558390.
2. Kelley D, Rinn J. Transposable elements reveal a stem cell-specific class of long noncoding RNAs. *Genome Biol*. 2012;13(11):R107. Epub 2012/11/28. doi: 10.1186/gb-2012-13-11-r107. PubMed PMID: 23181609; PubMed Central PMCID: PMC3580499.
3. Fuchs NV, Loewer S, Daley GQ, Izsak Z, Lower J, Lower R. Human endogenous retrovirus K (HML-2) RNA and protein expression is a marker for human embryonic and induced pluripotent stem cells. *Retrovirology*. 2013;10:115. Epub 2013/10/26. doi: 10.1186/1742-4690-10-115. PubMed PMID: 24156636; PubMed Central PMCID: PMC3819666.
4. Mager DL, Freeman JD. HERV-H endogenous retroviruses: presence in the New World branch but amplification in the Old World primate lineage. *Virology*. 1995;213(2):395-404. Epub 1995/11/10. doi: 10.1006/viro.1995.0012. PubMed PMID: 7491764.
5. Jern P, Sperber GO, Ahlsen G, Blomberg J. Sequence variability, gene structure, and expression of full-length human endogenous retrovirus H. *Journal of virology*. 2005;79(10):6325-37. Epub 2005/04/29. doi: 10.1128/JVI.79.10.6325-6337.2005. PubMed PMID: 15858016; PubMed Central PMCID: PMC1091717.
6. Jern P, Sperber GO, Blomberg J. Definition and variation of human endogenous retrovirus H. *Virology*. 2004;327(1):93-110. Epub 2004/08/26. doi: 10.1016/j.virol.2004.06.023. PubMed PMID: 15327901.
7. Goke J, Lu X, Chan YS, Ng HH, Ly LH, Sachs F, et al. Dynamic transcription of distinct classes of endogenous retroviral elements marks specific populations of early human embryonic cells. *Cell stem cell*. 2015;16(2):135-41. Epub 2015/02/07. doi: 10.1016/j.stem.2015.01.005. PubMed PMID: 25658370.
8. Wang J, Xie G, Singh M, Ghanbarian AT, Rasko T, Svetnik A, et al. Primate-specific endogenous retrovirus-driven transcription defines naive-like stem cells. *Nature*. 2014. Epub 2014/10/16. doi: 10.1038/nature13804. PubMed PMID: 25317556.
9. Lu X, Sachs F, Ramsay L, Jacques PE, Goke J, Bourque G, et al. The retrovirus HERVH is a long noncoding RNA required for human embryonic stem cell identity. *Nat Struct Mol Biol*. 2014;21(4):423-5. Epub 2014/04/01. doi: 10.1038/nsmb.2799. PubMed PMID: 24681886.
10. Ohnuki M, Tanabe K, Sutou K, Teramoto I, Sawamura Y, Narita M, et al. Dynamic regulation of human endogenous retroviruses mediates factor-induced reprogramming and differentiation potential. *Proceedings of the National Academy of Sciences of the United States of America*. 2014. Epub 2014/08/07. doi: 10.1073/pnas.1413299111. PubMed PMID: 25097266.
11. Friedli M, Turelli P, Kapopoulou A, Rauwel B, Castro-Diaz N, Rowe HM, et al. Loss of transcriptional control over endogenous retroelements during reprogramming to pluripotency. *Genome research*. 2014. Epub 2014/06/01. doi: 10.1101/gr.172809.114. PubMed PMID: 24879558.

495 12. Takahashi K, Tanabe K, Ohnuki M, Narita M, Ichisaka T, Tomoda K, et al. Induction of pluripotent stem
496 cells from adult human fibroblasts by defined factors. *Cell*. 2007;131(5):861-72. PubMed PMID: 18035408.

497 13. Takahashi K, Yamanaka S. Induction of pluripotent stem cells from mouse embryonic and adult fibroblast
498 cultures by defined factors. *Cell*. 2006;126(4):663-76. PubMed PMID: 16904174.

499 14. Yu J, Vodyanik MA, Smuga-Otto K, Antosiewicz-Bourget J, Frane JL, Tian S, et al. Induced pluripotent
500 stem cell lines derived from human somatic cells. *Science (New York, NY)*. 2007;318(5858):1917-20. PubMed
501 PMID: 18029452.

502 15. Koyanagi-Aoi M, Ohnuki M, Takahashi K, Okita K, Noma H, Sawamura Y, et al. Differentiation-defective
503 phenotypes revealed by large-scale analyses of human pluripotent stem cells. *Proceedings of the National
504 Academy of Sciences of the United States of America*. 2013. Epub 2013/11/22. doi: 10.1073/pnas.1319061110.
505 PubMed PMID: 24259714.

506 16. Loewer S, Cabili MN, Guttman M, Loh YH, Thomas K, Park IH, et al. Large intergenic non-coding RNA-
507 RoR modulates reprogramming of human induced pluripotent stem cells. *Nature genetics*. 2010;42(12):1113-7.
508 Epub 2010/11/09. doi: 10.1038/ng.710. PubMed PMID: 21057500; PubMed Central PMCID: PMC3040650.

509 17. Ng SY, Johnson R, Stanton LW. Human long non-coding RNAs promote pluripotency and neuronal
510 differentiation by association with chromatin modifiers and transcription factors. *The EMBO journal*. 2012;31(3):522-
511 33. Epub 2011/12/24. doi: 10.1038/emboj.2011.459. PubMed PMID: 22193719; PubMed Central PMCID:
512 PMCPMC3273385.

513 18. Zhao M, Ren C, Yang H, Feng X, Jiang X, Zhu B, et al. Transcriptional profiling of human embryonic stem
514 cells and embryoid bodies identifies HESRG, a novel stem cell gene. *Biochemical and biophysical research
515 communications*. 2007;362(4):916-22. Epub 2007/09/07. doi: 10.1016/j.bbrc.2007.08.081. PubMed PMID:
516 17803967.

517 19. Li G, Ren C, Shi J, Huang W, Liu H, Feng X, et al. Identification, expression and subcellular localization
518 of ESRG. *Biochemical and biophysical research communications*. 2013;435(1):160-4. Epub 2013/05/01. doi:
519 10.1016/j.bbrc.2013.04.062. PubMed PMID: 23628413.

520 20. Rand TA, Sutou K, Tanabe K, Jeong D, Nomura M, Kitaoka F, et al. MYC Releases Early Reprogrammed
521 Human Cells from Proliferation Pause via Retinoblastoma Protein Inhibition. *Cell reports*. 2018;23(2):361-75. Epub
522 2018/04/12. doi: 10.1016/j.celrep.2018.03.057. PubMed PMID: 29641997.

523 21. Takashima Y, Guo G, Loos R, Nichols J, Ficz G, Krueger F, et al. Resetting transcription factor control
524 circuitry toward ground-state pluripotency in human. *Cell*. 2014;158(6):1254-69. Epub 2014/09/13. doi:
525 10.1016/j.cell.2014.08.029. PubMed PMID: 25215486; PubMed Central PMCID: PMC4162745.

526 22. Theunissen TW, Powell BE, Wang H, Mitalipova M, Faddah DA, Reddy J, et al. Systematic identification
527 of culture conditions for induction and maintenance of naive human pluripotency. *Cell stem cell*. 2014;15(4):471-87.
528 Epub 2014/08/05. doi: 10.1016/j.stem.2014.07.002. PubMed PMID: 25090446; PubMed Central PMCID:
529 PMC4184977.

530 23. Guo G, von Meyenn F, Rostovskaya M, Clarke J, Dietmann S, Baker D, et al. Epigenetic resetting of
531 human pluripotency. *Development* (Cambridge, England). 2017;144(15):2748-63. Epub 2017/08/03. doi:
532 10.1242/dev.146811. PubMed PMID: 28765214; PubMed Central PMCID: PMCPMC5560041.

533 24. Di Stefano B, Ueda M, Sabri S, Brumbaugh J, Huebner AJ, Sahakyan A, et al. Reduced MEK inhibition
534 preserves genomic stability in naive human embryonic stem cells. *Nature methods*. 2018;15(9):732-40. Epub
535 2018/08/22. doi: 10.1038/s41592-018-0104-1. PubMed PMID: 30127506; PubMed Central PMCID:
536 PMCPMC6127858.

537 25. Collier AJ, Panula SP, Schell JP, Chovanec P, Plaza Reyes A, Petropoulos S, et al. Comprehensive Cell
538 Surface Protein Profiling Identifies Specific Markers of Human Naive and Primed Pluripotent States. *Cell stem cell*.
539 2017;20(6):874-90.e7. Epub 2017/03/28. doi: 10.1016/j.stem.2017.02.014. PubMed PMID: 28343983; PubMed
540 Central PMCID: PMCPMC5459756.

541 26. Takahashi K, Jeong D, Wang S, Narita M, Jin X, Iwasaki M, et al. Critical Roles of Translation Initiation
542 and RNA Uridylation in Endogenous Retroviral Expression and Neural Differentiation in Pluripotent Stem Cells. *Cell reports*.
543 2020;31(9):107715. Epub 2020/06/04. doi: 10.1016/j.celrep.2020.107715. PubMed PMID: 32492424.

544 27. Chambers SM, Fasano CA, Papapetrou EP, Tomishima M, Sadelain M, Studer L. Highly efficient
545 neural conversion of human ES and iPS cells by dual inhibition of SMAD signaling. *Nature biotechnology*.
546 2009;27(3):275-80.

547 28. Doi D, Samata B, Katsukawa M, Kikuchi T, Morizane A, Ono Y, et al. Isolation of human induced pluripotent
548 stem cell-derived dopaminergic progenitors by cell sorting for successful transplantation. *Stem cell reports*.
549 2014;2(3):337-50. Epub 2014/03/29. doi: 10.1016/j.stemcr.2014.01.013. PubMed PMID: 24672756; PubMed
550 Central PMCID: PMC3964289.

551 29. Nakagawa M, Koyanagi M, Tanabe K, Takahashi K, Ichisaka T, Aoi T, et al. Generation of induced
552 pluripotent stem cells without Myc from mouse and human fibroblasts. *Nature biotechnology*. 2008;26(1):101-6.
553 PubMed PMID: 18059259.

554 30. Wernig M, Meissner A, Cassady JP, Jaenisch R. c-Myc is dispensable for direct reprogramming of mouse
555 fibroblasts. *Cell stem cell*. 2008;2(1):10-2. Epub 2008/03/29. doi: S1934-5909(07)00315-3 [pii]
556 10.1016/j.stem.2007.12.001. PubMed PMID: 18371415.

557 31. Smith KN, Starmer J, Miller SC, Sethupathy P, Magnuson T. Long Noncoding RNA Moderates MicroRNA
558 Activity to Maintain Self-Renewal in Embryonic Stem Cells. *Stem cell reports*. 2017;9(1):108-21. Epub 2017/06/06.
559 doi: 10.1016/j.stemcr.2017.05.005. PubMed PMID: 28579393; PubMed Central PMCID: PMCPMC5511051.

560 32. Hunkler HJ, Hoepfner J, Huang CK, Chatterjee S, Jara-Avaca M, Gruh I, et al. The Long Non-coding RNA
561 Cyrano Is Dispensable for Pluripotency of Murine and Human Pluripotent Stem Cells. *Stem cell reports*.
562 2020;15(1):13-21. Epub 2020/06/13. doi: 10.1016/j.stemcr.2020.05.011. PubMed PMID: 32531193; PubMed
563 Central PMCID: PMCPMC7363876.

564 33. Gilbert LA, Larson MH, Morsut L, Liu Z, Brar GA, Torres SE, et al. CRISPR-mediated modular RNA-guided

565 regulation of transcription in eukaryotes. *Cell.* 2013;154(2):442-51. Epub 2013/07/16. doi:
566 10.1016/j.cell.2013.06.044. PubMed PMID: 23849981; PubMed Central PMCID: PMCPMC3770145.

567 34. Mandegar MA, Huebsch N, Frolov EB, Shin E, Truong A, Olvera MP, et al. CRISPR Interference Efficiently
568 Induces Specific and Reversible Gene Silencing in Human iPSCs. *Cell stem cell.* 2016;18(4):541-53. Epub
569 2016/03/15. doi: 10.1016/j.stem.2016.01.022. PubMed PMID: 26971820; PubMed Central PMCID:
570 PMCPMC4830697.

571 35. Lennox KA, Behlke MA. Cellular localization of long non-coding RNAs affects silencing by RNAi more than
572 by antisense oligonucleotides. *Nucleic acids research.* 2016;44(2):863-77. Epub 2015/11/19. doi:
573 10.1093/nar/gkv1206. PubMed PMID: 26578588; PubMed Central PMCID: PMCPMC4737147.

574 36. Liu SJ, Lim DA. Modulating the expression of long non-coding RNAs for functional studies. *EMBO reports.*
575 2018;19(12). Epub 2018/11/24. doi: 10.15252/embr.201846955. PubMed PMID: 30467236; PubMed Central
576 PMCID: PMCPMC6280642.

577 37. Izsvák Z, Wang J, Singh M, Mager DL, Hurst LD. Pluripotency and the endogenous retrovirus HERVH:
578 Conflict or serendipity? *BioEssays : news and reviews in molecular, cellular and developmental biology.*
579 2016;38(1):109-17. Epub 2016/01/07. doi: 10.1002/bies.201500096. PubMed PMID: 26735931.

580 38. Sekine K, Tsuzuki S, Yasui R, Kobayashi T, Ikeda K, Hamada Y, et al. Robust detection of undifferentiated
581 iPSC among differentiated cells. *Scientific reports.* 2020;10(1):10293. Epub 2020/06/26. doi: 10.1038/s41598-020-
582 66845-6. PubMed PMID: 32581272; PubMed Central PMCID: PMCPMC7314783 conflict of interest.

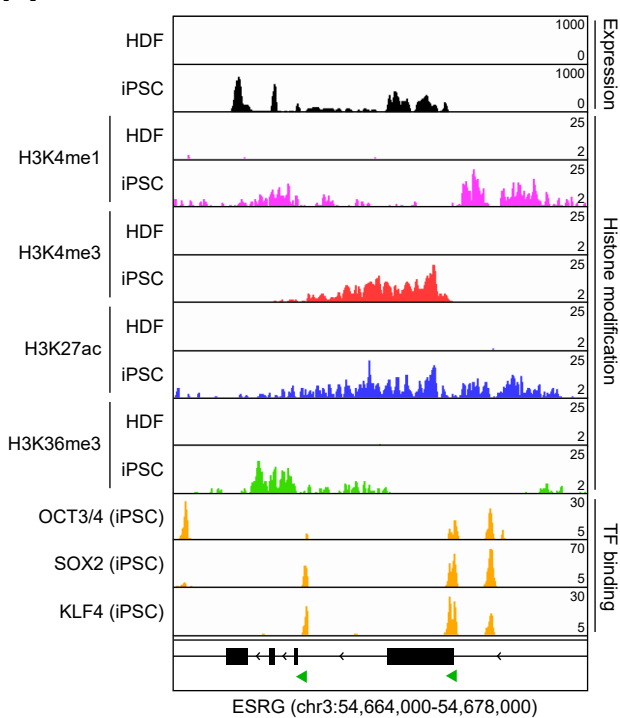
583 39. Morita S, Kojima T, Kitamura T. Plat-E: an efficient and stable system for transient packaging of
584 retroviruses. *Gene Ther.* 2000;7(12):1063-6. PubMed PMID: 10871756.

585

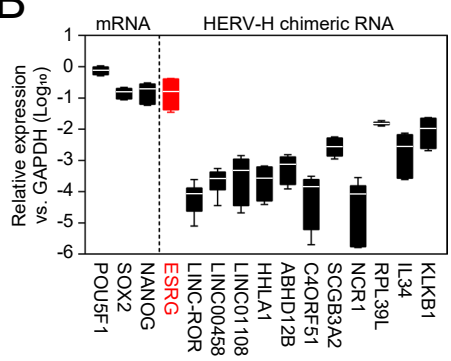
586

Fig. 1

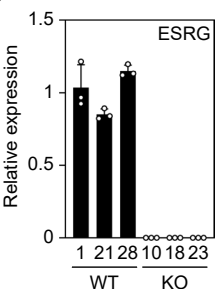
A



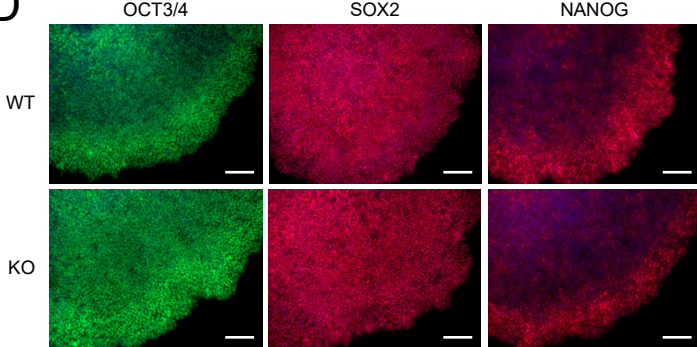
B



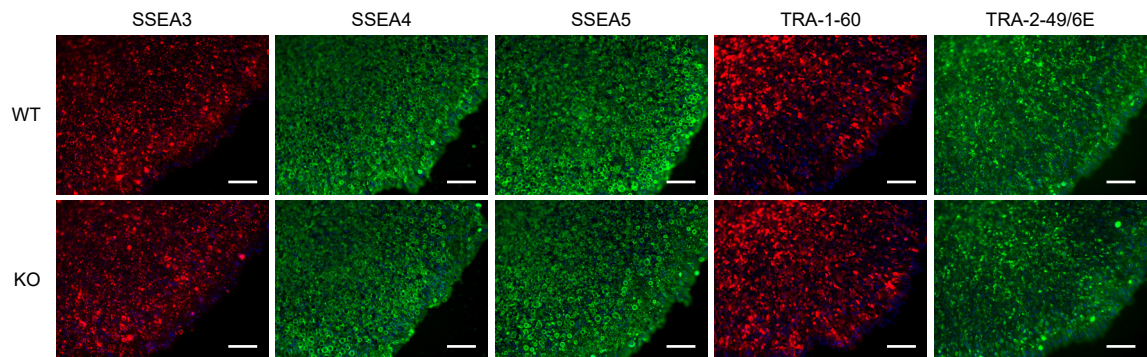
C



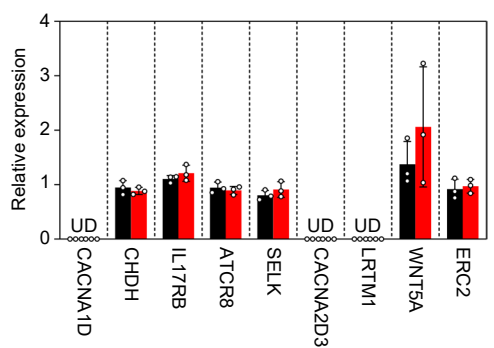
D



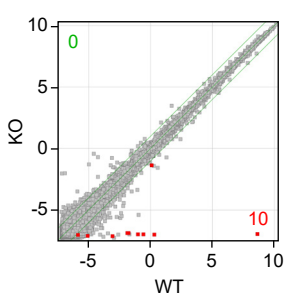
E



F



G



H

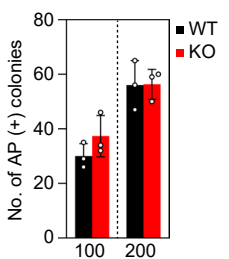


Fig. 2

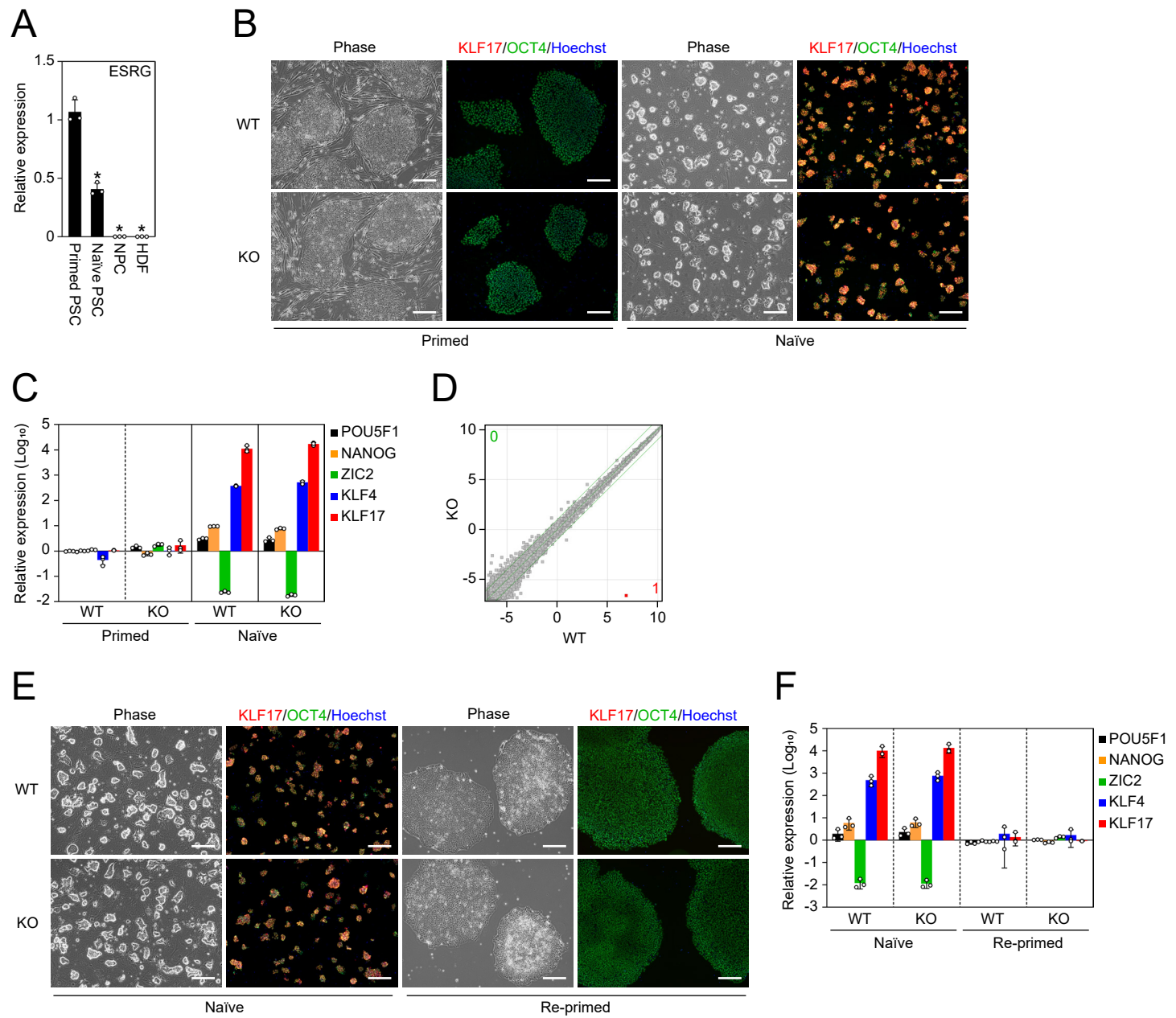


Fig. 3

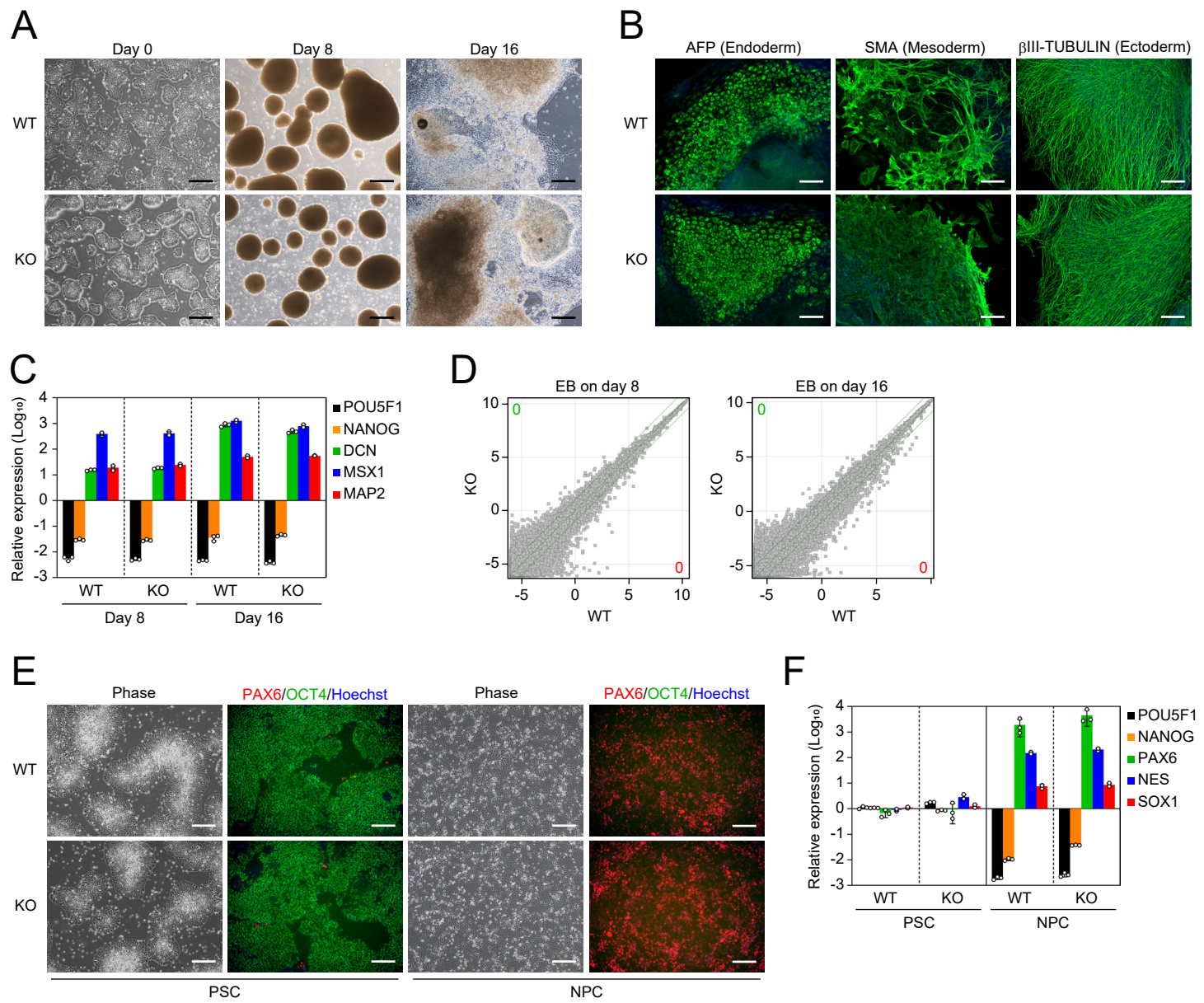
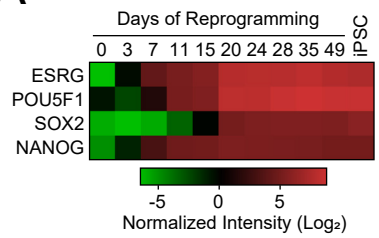
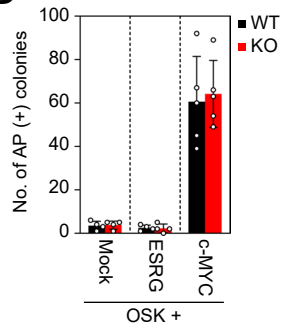


Fig. 4

A

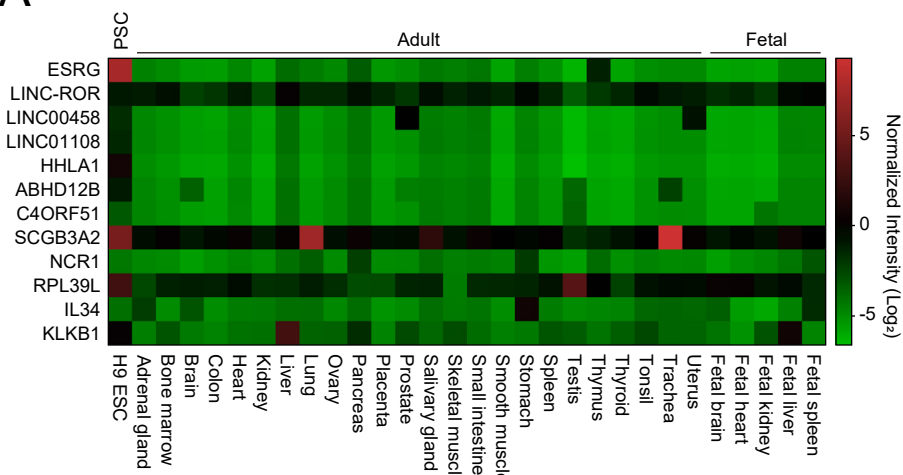


B

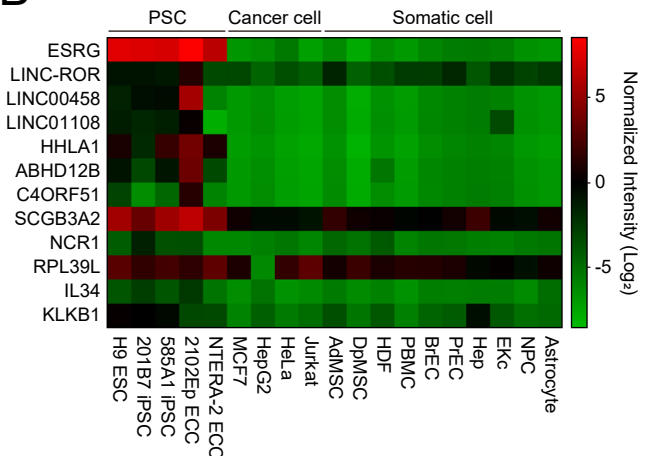


S1 Fig.

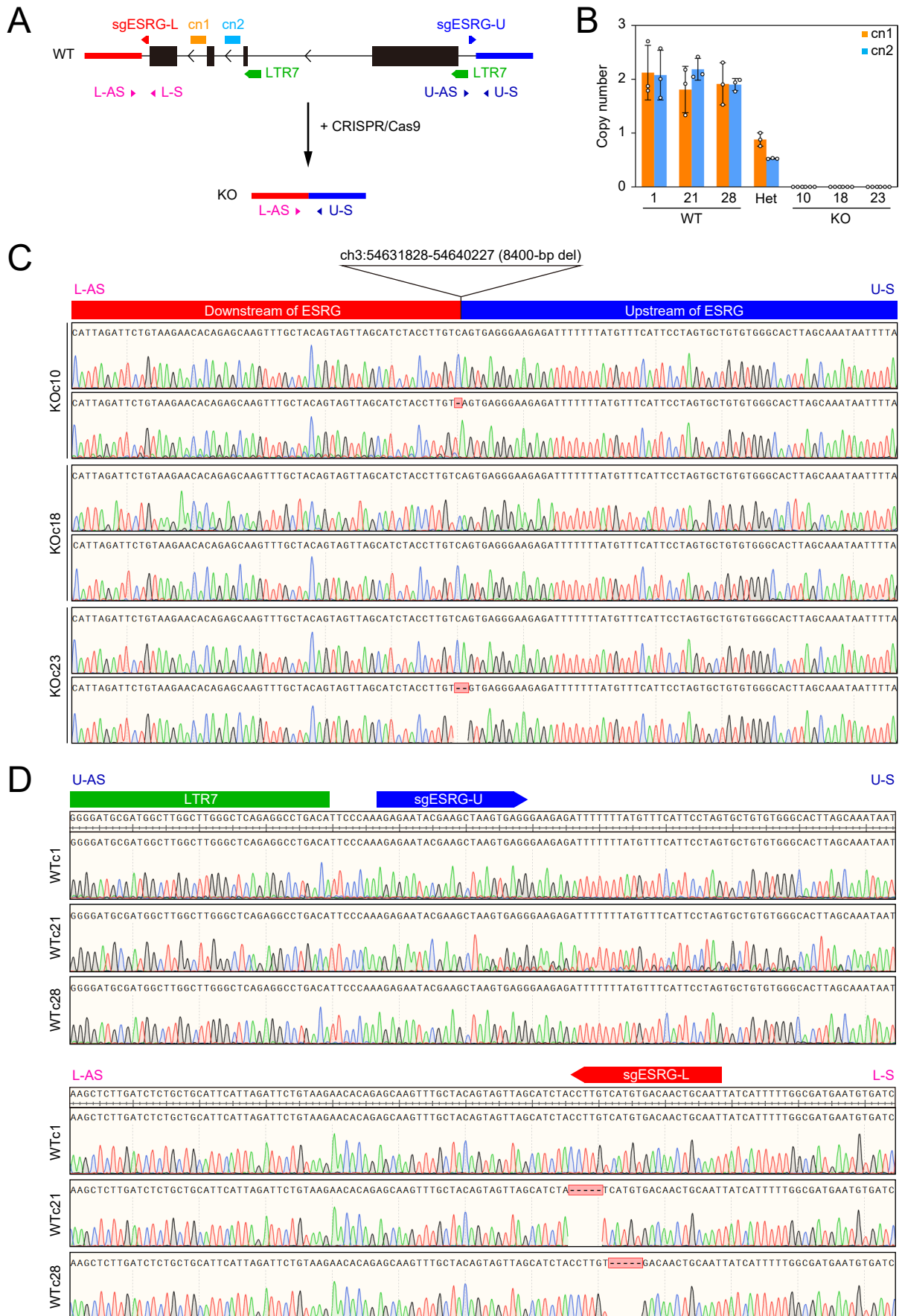
A



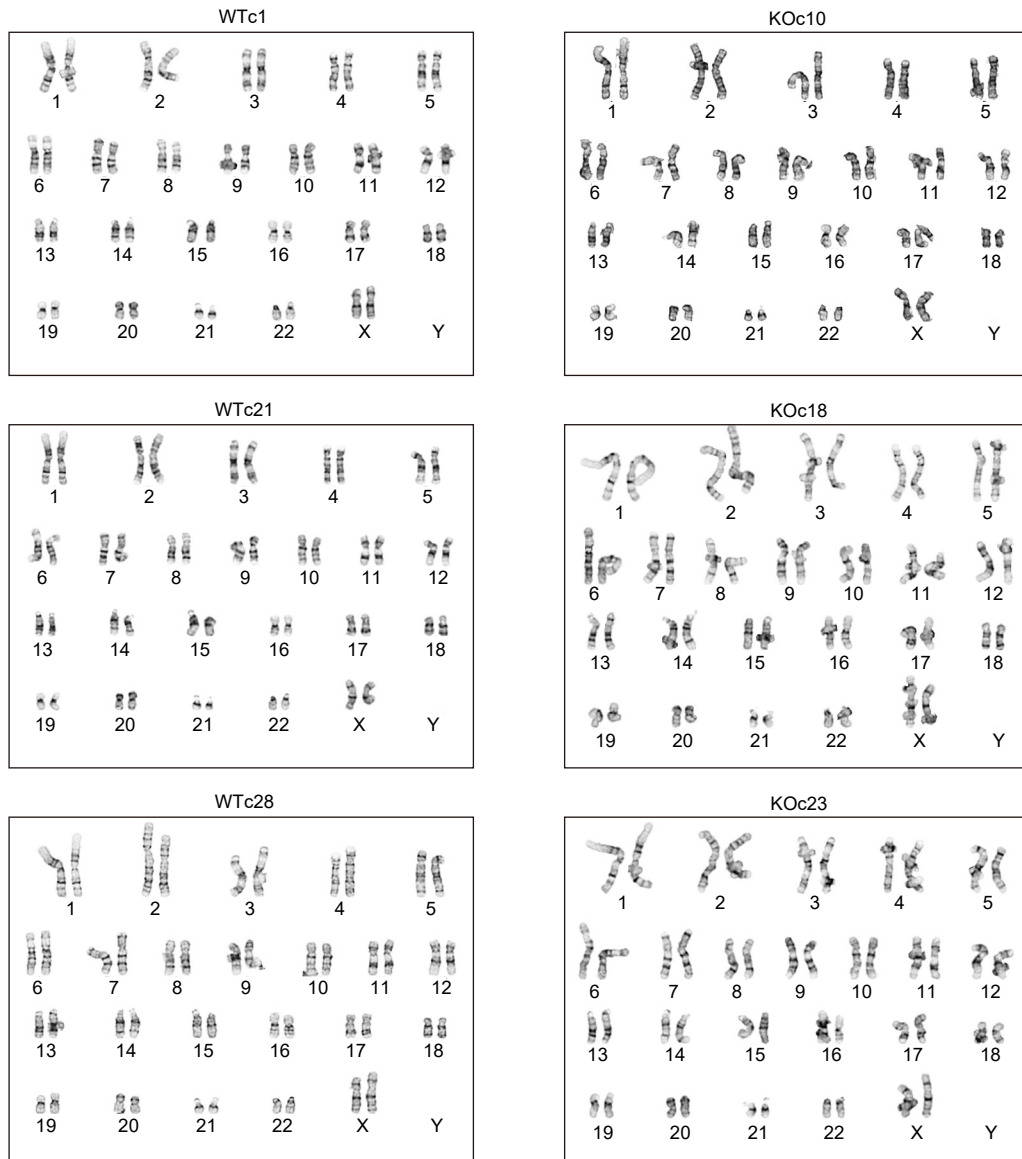
B



S2 Fig.



S3 Fig.



S1 Table. Primers used in this study

Name	Sequence (5' to 3')
ESRG-U-S	ACAATTACATGTCAATGCTGCGAG
ESRG-U-AS	GTGGAATGTCATCAGTTAAGGTGG
ESRG-L-S	CACTGCAAAGATCACATTCATCGC
ESRG-L-AS	GGCTGGAGCTTAGAATGGTCAG
ESRG-BamH1-S	AGTTAATTAAAGGATCCGCTGACTCTCTTCGGACTCAGC
ESRG-Not1-AS	ACTGTGCTGGCGGCCGCACTCATCAAACCATTGAATTAAATTGC

S2 Table. TaqMan Assays used in this study

Target	Assay ID
ESRG	Hs03666618_s1
LINC-ROR	Hs04332550_m1
LINC00458	Hs05005988_m1
LINC01108	Hs04402672_m1
HHLA1	Hs00903176_g1
ABHD12B	Hs00997975_g1
C4ORF51	Hs03037752_m1
SCGB3A2	Hs00369678_m1
NCR1	Hs00950813_m1
RPL39L	Hs01027925_m1
IL34	Hs01050928_g1
KLKB1	Hs00168478_m1
POU5F1	Hs04260367_gH
SOX2	Hs01053409_s1
NANOG	Hs02387400_g1
ZIC2	Hs00600845_m1
KLF4	Hs00358836_m1
KLF17	Hs00702999_m1
PAX6	Hs00240871_m1
NES	Hs04187831_g1
SOX1	Hs01057642_s1
GAPDH	Hs02786624_g1